Low-Latency Robust MPC for CACC under Variable Road Geometry ⋆

Jianglin Lan *, Dezong Zhao * and Daxin Tian **

*Department of Aeronautical and Automotive Engineering,
Loughborough University, Loughborough LE11 3TU, United Kingdom
(e-mails: j.lan@lboro.ac.uk, d.zhao@lboro.ac.uk).
** School of Transportation Science and Engineering, Beihang
University, Beijing 100191, China (e-mail: dtian@buaa.edu.cn).

Abstract: Cooperative adaptive cruise control (CACC) has attracted much research attention, due to its great potential in improving traffic throughput, safety and energy efficiency. This paper aims to address the following problems that are rarely investigated in the literature: (i) the time delay caused by online computation of the optimal control action, and (ii) robustly stable CACC under variable road geometry. To this end, a one-step ahead robust model predictive control (MPC) is developed for achieving CACC and lane keeping (LK) of the followers in the platoon, by leveraging vehicle-to-vehicle (V2V) and vehicle-to-infrastructure (V2I) communications. In the proposed design, the current MPC policy is generated one-step ahead during the previous sampling period to avoids the optimization-induced time delay existing in the traditional MPC. LK control is incorporated with CACC to ensure vehicle lateral stability and vehicle following under variable road geometry. The MPC design is formulated as an easily solved linear matrix inequality (LMI) optimization problem with consideration of the control input limits and constraints on platooning errors and lateral displacement. Effectiveness of the proposed MPC and its advantages over the traditional MPC are verified by simulating a vehicle platoon on roads with time-varying bank, curvature and grade.

Keywords: Cooperative adaptive cruise control, lane keeping, predictive control, road geometry, time delay.

1. INTRODUCTION

Cooperative adaptive cruise control (CACC) is deployed for vehicle platooning to improve traffic capacity, safety and fuel economy, using vehicle-to-vehicle (V2V) and/or vehicle-to-infrastructure (V2I) communications. The goal of CACC is controlling the followers in the platoon to track the leader velocity, whilst maintaining a safe inter-vehicle distance. Multiple CACC approaches have been developed, among which model predictive control (MPC) has been widely used because its remarkable ability of optimally controlling the vehicles under physical and safety constraints (Guanetti et al., 2018).

The existing MPC approach (termed as real-time MPC in this paper), including the robust MPC (Zhang et al., 2012) and tube MPC (Feng et al., 2019; van Nunen et al., 2019), implements the online optimization and control action sequentially. For each follower, at each time instant, the optimization is initiated by the obtained real-time state information including (i) its own velocity and the inter-vehicle distance measured by onboard sensors, and (ii) the velocities and accelerations of the preceding vehicle and/or leader transmitted by V2V communication

(Feng et al., 2019; van Nunen et al., 2019). The follower needs to wait for the control action during the period of data collection and computation. This waiting time is usually ignored in the literature and the control action is assumed to be applied instantaneously. However, the waiting time will be non-negligible for high-speed driving vehicles. The delay can be large enough to influence the implementation of MPC in real-time and lead to control performance degradation or even control failure (Findeisen and Allgöwer, 2004). This is the motivation of developing a new CACC strategy to reduce the time delay. Particularly, this paper focuses on proposing a new MPC approach to avoid the optimization-induced delay, while reducing the delay caused by data collection is not covered.

A one-step ahead MPC is to be proposed in this work using a concept like the advanced-step MPC (Zavala and Biegler, 2009). The key idea is to solve the future optimization problem in advance during the current sampling period, by using the current control action to predict the future vehicle system state. The control action is applied to the vehicle once the real-time state information is collected, which avoids the optimization-induced latency. Different from the tube MPC (Feng et al., 2019; van Nunen et al., 2019) and advanced-step MPC (Zavala and Biegler, 2009), the MPC optimization in this paper is formulated as a linear matrix inequality (LMI) problem, which can be solved more efficiently and is easier in incorporating sys-

tem uncertainty and disturbance. It is worth noting that the proposed one-step ahead MPC requires more online computation than the *explicit* MPC where the control laws are calculated fully offline (Gupta and Falcone, 2018). However, *explicit* MPC usually has degraded control performance because it is very complex to generate the exact control solutions to cover the entire operating space.

Another rarely studied problem in the literature is designing CACC under variable road geometry. Most existing works investigate vehicles in straight and flat lanes via controlling the longitudinal dynamics of the followers only (Guanetti et al., 2018). This is inapplicable for CACC under variable road geometry, because the vehicle longitudinal stability is affected by road bank and curvature, while the lateral stability is affected by road grade (Rajamani, 2011). Moreover, there is nonlinear coupling between the longitudinal and lateral dynamics. Hence, it is necessary to combine lane keeping (LK) with CACC to achieve robustly stable vehicle platooning (Attia et al., 2012). The combined design of LK and CACC for vehicles on curved roads is studied in Xu et al. (2019); Zhang et al. (2012). The road grade preview is used in Firoozi et al. (2019) to improve driving comfort and fuel efficiency. This paper considers LK and CACC on more realistic roads with time-varying bank, curvature and grade.

In this paper, a one-step ahead robust MPC approach is developed for achieving robustly stable CACC and LK, by confining the errors of vehicle following and lane keeping within robustly positive invariant (RPI) sets (Blanchini and Miani, 2008). The CACC and LK controllers are obtained following the same design procedure based on an easily solved LMI formulation. To handle nonlinearity of the lateral tracking error system under time-varying longitudinal velocity, the LK design is based on a linear parameter varying (LPV) modelling. The proposed CACC and LK designs exploit V2V communication to obtain the real-time acceleration of the preceding vehicle, and V2I communication to access information of road curvature and grade. Unlike the existing designs (Feng et al., 2019; Firoozi et al., 2019; van Nunen et al., 2019), no predicted acceleration or road preview is used in the proposed design.

The rest of this paper is organized as follows. Section 2 describes the system models and the design problem. Section 3 presents the one-step ahead robust MPC design. Section 4 provides simulation of a vehicle platoon under variable road geometry. Section 5 draws conclusions.

2. PROBLEM DESCRIPTION

For simplicity and clarity, a two-vehicle platooning system is used to illustrate the key ideas of the proposed design. The design is directly applicable for platooning multiple vehicles by regarding each two consecutive vehicles as a two-vehicle platooning system (with the predecessor as the leader). To demonstrate this, a case study of platooning three vehicles is provided in Section 4.

For the two-vehicle platooning system, only the position, velocity and acceleration of the leader need to be known. Hence, the following point-mass system is widely used to represent the leader (Guanetti et al., 2018):

$$\begin{bmatrix} \dot{p}^l \\ \dot{v}^l \end{bmatrix} = \begin{bmatrix} 0 & 1 \\ 0 & 0 \end{bmatrix} \begin{bmatrix} p^l \\ v^l \end{bmatrix} + \begin{bmatrix} 0 \\ 1 \end{bmatrix} a^l \qquad (1)$$

where p^l, v^l and a^l are the vehicle position, velocity and acceleration, respectively.

To design CACC under variable road geometry, both the longitudinal and lateral dynamics of the follower are considered. The longitudinal dynamics are represented by

$$\begin{bmatrix} \dot{p} \\ \dot{v} \end{bmatrix} = \begin{bmatrix} 0 & 1 \\ 0 & 0 \end{bmatrix} \begin{bmatrix} p \\ v \end{bmatrix} + \begin{bmatrix} 0 \\ 1/m \end{bmatrix} (\varphi - f - \bar{d}) \qquad (2)$$

where p, v and φ are the vehicle position, velocity and desired torque, respectively; f represents the known system disturbance defined as $f = \hat{F}_{\text{drag}} + F_{\text{roll}} + F_{\text{gravity}} - F_{\text{lateral}}$, with the approximated aerodynamic drag $\hat{F}_{\text{drag}} = 0.5 C_d \rho_{\text{air}} A_f v^2$ and the approximation error $\bar{d} = 0.5 C_d \rho A_f (v + v_{\text{wind}})^2 - \hat{F}_{\text{drag}}$; $F_{\text{roll}} = mg\mu \cos(\beta)$ and $F_{\text{gravity}} = mg \sin(\beta)$ represent the rolling resistance and gravitational force, respectively; $F_{\text{lateral}} = m\dot{y}\dot{\psi}$ represents the influence from the lateral dynamics; C_d is the drag coefficient; ρ_{air} is the air density; A_f is the frontal area; v_{wind} is the longitudinal component of the wind speed; m is the vehicle mass; g is the gravitational acceleration; μ is the rolling resistance coefficient; β is the road grade; $\dot{y}$ is the lateral velocity and $\dot{\psi}$ is the yaw rate. Since v and v_{wind} are bounded, there exist positive constants $\bar{d}_{\text{max}}$ and f_{max} satisfying $|\bar{d}| \leq \bar{d}_{\text{max}}$ and $|f| \leq f_{\text{max}}$, respectively.

Define the vehicle following errors as $\Delta p = p^l - p - d_r$ and $\Delta v = v^l - v$, where d_r is the safe inter-vehicle distance. By using (1) and (2), the CACC system is represented by

$$\dot{\chi} = \mathcal{A}\chi + \mathcal{B}\varphi + \mathcal{E}(\bar{\rho} + \bar{d}) \qquad (3)$$

where $\chi = \begin{bmatrix} \Delta p \\ \Delta v \end{bmatrix}$, $\mathcal{A} = \begin{bmatrix} 0 & 1 \\ 0 & 0 \end{bmatrix}$, $\mathcal{B} = \begin{bmatrix} 0 \\ -1/m \end{bmatrix}$, $\mathcal{E} = -\mathcal{B}$ and $\bar{\rho} = ma^l + f$.

The lateral tracking error system of the follower is given as (Rajamani, 2011)

$$\dot{x} = A(v)x + B_c\delta + E(v)\rho + D_c d \qquad (4)$$

where $x = [e_y \ \dot{e}_y \ e_\psi \ \dot{e}_\psi]^\top$ is the state with e_y and e_ψ denoting the lateral displacement and yaw angle error with respect to the road, respectively; δ is the front wheel steering angle; $\rho = \dot{\psi}_{\text{des}} = v/R$ is the desired yaw rate calculated from longitudinal velocity v and road radius R; $d = \sin(\theta)$ denotes the influence of road bank angle θ. The system matrices are given as

$$A = \begin{bmatrix} 0 & 1 & 0 & 0 \\ 0 & -\dfrac{2(c_f + c_r)}{mv} & \dfrac{2(c_f + c_r)}{m} & \dfrac{2(c_r l_r - c_f l_f)}{mv} \\ 0 & 0 & 0 & 1 \\ 0 & \dfrac{2(c_r l_r - c_f l_f)}{I_z v} & \dfrac{2(c_f l_f - c_r l_r)}{I_z} & -\dfrac{2(c_f l_f^2 + c_r l_r^2)}{I_z v} \end{bmatrix},$$

$$B_c = \begin{bmatrix} 0 \\ \dfrac{2c_f}{m} \\ 0 \\ \dfrac{2c_f l_f}{I_z} \end{bmatrix}, \ E = \begin{bmatrix} 0 \\ \dfrac{2(c_r l_r - c_f l_f)}{mv} - v \\ 0 \\ -\dfrac{2(c_f l_f^2 + c_r l_r^2)}{I_z v} \end{bmatrix}, \ D_c = \begin{bmatrix} 0 \\ g \\ 0 \\ 0 \end{bmatrix}$$

where c_f and c_r are the cornering stiffness of the front and rear tires, respectively; l_f and l_r are the distances from the

center of gravity of the vehicle to the front and rear tires, respectively; I_z is the yaw moment of inertia.

The CACC system (3) is perturbed by the leader acceleration, aerodynamic drag, rolling resistance and gravitational force, while the LK system (4) is perturbed by road bank and curvature. Theses disturbances affect vehicle stability and should be considered in the control design. Moreover, there exists nonlinear coupling between the CACC and LK systems, which should also be considered in the design. The simultaneous synthesis of CACC and LK controllers is difficult due to the nonlinear dynamics coupling. Hence, they will be designed separately in this paper with robustness against the disturbances and coupling. By using V2V and V2I communications, the real-time leader acceleration, road grade and curvature are accessible. They are used in the CACC and LK controllers to compensate their effects. However, the approximation error of aerodynamic drag ($\bar{d}$) and the road bank angle are assumed to be unknown, whose effects are to be attenuated. The physical limitations of φ and δ also need to be considered in the design to guarantee vehicle safety.

In summary, the goals of designing CACC and LK controllers based on (3) and (4) include system stability, robustness and satisfaction of physical limitations. Moreover, constraints need to be imposed on the inter-vehicle distance error Δp and the lateral displacement e_y to guarantee good car following and lane keeping. In order to improve the control performance, the proposed controller should avoid the optimization-induced time delay exiting in the traditional real-time MPC. All these goals can be realized by developing one-step ahead robust MPC controllers, as detailed in the next section.

3. CACC AND LK DESIGNS

The key idea of the proposed one-step ahead robust MPC is compared with that of the real-time MPC in Fig. 1, where $k \geq 1$ is the sampling instance and the optimization is assumed to accomplish within one sampling period. It is seen that for the one-step ahead MPC, the optimization task for generating the controller $u(k)$ is shifted to the previous sampling period $k-1$, which thus avoids the waiting time caused by the optimization. Details of designing one-step ahead robust MPC controllers for achieving LK and CACC are given in Sections 3.1 and 3.2, respectively.

3.1 LK Controller Design

Since the road curvature R is known, the desired yaw rate $\rho = v/R$ is known and its effect on the lateral dynamics can be compensated. However, it is seen from (4) that ρ cannot be completely compensated via δ because $\mathrm{rank}([B_c\ E(v)]) \neq \mathrm{rank}(B_c)$. Hence, the term $E(v)\rho$ is partitioned as

$$E(v)\rho = -B_c\hat{\rho} + (E(v) + l_f/vB_c)\rho \tag{5}$$

where the part $\hat{\rho} = l_f\rho/v = l_f/R$ can be compensated. To remove steady-state offset of the lateral displacement, the integral $\int e_y \mathrm{d}t$ will be used in the proposed controller. By defining $\hat{x} = [x^\top \int e_y \mathrm{d}t]^\top$ and using (5), the system (4) is reformulated as

$$\dot{\hat{x}} = \hat{A}(v)\hat{x} + \hat{B}_c(\delta - \hat{\rho}) + \hat{D}(v)w \tag{6}$$
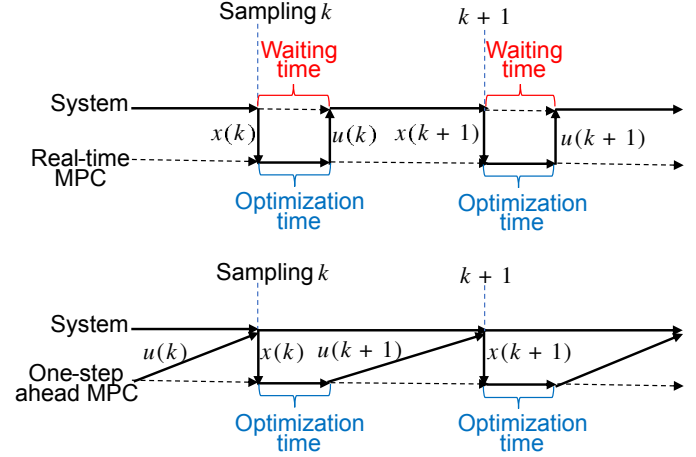
Fig. 1. Comparison of real-time and one-step ahead MPCs

where

$$\hat{A}(v) = \begin{bmatrix} A(v) & 0 \\ \Lambda & 0 \end{bmatrix}, \ \Lambda = [1\ 0\ 0\ 0], \ \hat{B}_c = \begin{bmatrix} B_c \\ 0 \end{bmatrix},$$

$$\hat{D} = \begin{bmatrix} 0 & 0 \\ 2c_r l_r/(mv) & g \\ 0 & 0 \\ -2c_r l_r^2/(I_z v) & 0 \\ 0 & 0 \end{bmatrix}, \ w = \begin{bmatrix} \rho \\ -v\rho/g + d \end{bmatrix}.$$

Since ρ, v and d are bounded, there is a positive constant $w_{\max}$ satisfying $\|w\|^2 \leq w_{\max}$. Assume that the longitudinal velocity v satisfies $v \in [v_{\min}, v_{\max}]$, where $v_{\min}$ and $v_{\max}$ are positive constants representing the minimum and maximum velocities, respectively. The case of $v = 0$ m/s is not considered in this paper. Define $\nu = 1/v$, then it holds that $\nu \in [\nu_{\min}, \nu_{\max}]$ with $\nu_{\min} = 1/v_{\max}$ and $\nu_{\max} = 1/v_{\min}$. Under the sampling time t_s, the system (6) is rewritten as a discrete-time LPV system

$$\hat{x}(k+1) = \hat{A}_\nu \hat{x}(k) + \hat{B}(\delta(k) - \hat{\rho}(k)) + \hat{D}_\nu w(k) \tag{7}$$

with the matrices given by

$$\hat{A}_\nu = \sum_{l=1}^{2} \alpha_l(k)\hat{A}_l, \ \hat{B} = t_s\hat{B}_c, \ \hat{D}_\nu = \sum_{l=1}^{2} \alpha_l(k)\hat{D}_l,$$

$$\alpha_1(k) = \frac{\nu(k) - \nu_{\min}}{\nu_{\max} - \nu_{\min}}, \ \alpha_2(k) = \frac{\nu_{\max} - \nu(k)}{\nu_{\max} - \nu_{\min}},$$

$$\hat{A}_1 = I_5 + t_s A(\nu_{\min}), \ \hat{A}_2 = I_5 + t_s A(\nu_{\max}),$$

$$\hat{D}_1 = t_s D(\nu_{\min}), \ \hat{D}_2 = t_s D(\nu_{\max}).$$

A one-step ahead robust MPC controller is to be designed for the system (7). One-step ahead robust MPC for LPV system is recently studied in Hu and Ding (2020). However, their design is conservative due to the use of a constant linear feedback controller and it is not for automotive application. In this paper, the following LPV controller combining feedback and feedforward is proposed:

$$\delta(i|k) = \begin{cases} F(k-1)\hat{x}(i|k) + \hat{\rho}(i|k), & i = 0 \\ F(k)\hat{x}(i|k) + \hat{\rho}(i|k), & \forall i > 0 \end{cases} \tag{8}$$

where $k \geq 1$ and $F(k) = \sum_{l=1}^{2} \alpha_l(i|k)F_{k,l}$ with the design gains $F_{k,l}$. The notation $\hat{x}(i|k)$ is used to present the predicted state at time $k+i$ based on the measured state $\hat{x}(k)$ at time k. As shown in Fig. 1, at time k, the controller $\delta(k)$ with the gain $F(k-1)$ obtained at time $k-1$ is applied to the system (7).

The controller (8) is designed to minimize the cost function

$$J_{\text{LK}}(k) = \sum_{i=1}^{\infty} \ell(i|k)$$

where $\ell(i|k) = \|\hat{x}(i|k)\|_Q^2 + \|\bar{\delta}(i|k)\|_S^2 - \lambda\|w(k+i)\|^2$ with the feedback control $\bar{\delta}(i|k) = F(k)\hat{x}(i|k)$; Q and S are given positive definite matrices; $\lambda > 0$ is a design variable.

The controller (8) is also designed to guarantee stability of the system (7) under the constraints $|\delta(k)| \leq \delta_{\max}$ and $|e_y(k)| \leq e_{y,\max}$, where $\delta_{\max}$ and $e_{y,\max}$ are the maximum steering angle and lateral displacement, respectively. Moreover, the state $\hat{x}(k)$ is confined within a robustly positive invariant (RPI) set. The RPI set for LPV system is defined as (Hu and Ding, 2020):

Definition 1. A set Ω is an RPI set for the LPV system

$$\hat{x}(k+1) = \sum_{l=1}^{2} \alpha_l(k)(\hat{A}_l\hat{x}(k) + \hat{D}_l w(k)),$$

if $\forall \hat{x}(k) \in \Omega$, $\hat{x}(k+1) \in \Omega$ holds for all $w(k)$ and for all $\alpha_l(k)$ satisfying $\alpha_l \geq 0$ and $\sum_{l=1}^{2} \alpha_l(k) = 1$.

Design of the controller (8) is formulated as the LMI optimization problem in Theorem 2.

Theorem 2. The system (7) under the controller (8) is robustly stable and satisfies $|\delta(k)| \leq \delta_{\max}$ and $|e_y(k)| \leq e_{y,\max}$, if the following optimization problem is feasible:

$$\min_{\gamma, X_l, G_l, Y_l, l \in [1,2]} \gamma$$

$$\begin{bmatrix} (1-\xi)(G_l^\top + G_l - X_l) & \star & \star & \star & \star \\ 0 & \xi w_{\max}^{-1} I & \star & \star & \star \\ \hat{A}_l G_l + \hat{B}Y_l & \hat{D}_l & X_j & \star & \star \\ Q^{1/2} & 0 & 0 & \gamma I & \star \\ S^{1/2}Y_l & 0 & 0 & 0 & \gamma I \end{bmatrix} \geq 0 \quad (9)$$

$$\begin{bmatrix} 1-\epsilon & \star & \star \\ 0 & \epsilon w_{\max}^{-1} I & \star \\ (\hat{A}_l + \hat{B}F_{k-1,l})\hat{x}(k) & \hat{D}_l & X_j \end{bmatrix} \geq 0 \quad (10)$$

$$\begin{bmatrix} \bar{\delta}_{\max}^2 I & \star \\ Y_l^\top & G_l^\top + G_l - X_l \end{bmatrix} \geq 0 \quad (11)$$

$$\begin{bmatrix} e_{y,\max}^2 I & \star & \star \\ (\hat{A}_l G_l + \hat{B}Y_l)^\top \Gamma^\top & X_l & \star \\ \hat{D}_l^\top \Gamma^\top & 0 & w_{\max}^{-1} I \end{bmatrix} \geq 0 \quad (12)$$

$$\gamma > 0, \quad X_l = X_l^\top > 0 \quad (13)$$

where $l, j \in [1,2]$ and $\Gamma = [1\ 0\ 0\ 0\ 0]$; $\xi, \epsilon \in (0,1]$; $\bar{\delta}_{\max}$ is the upper bound of $\bar{\delta}(k)$ defined as $\bar{\delta}_{\max} = \delta_{\max} - \hat{\rho}_{\max}$ with $\hat{\rho}_{\max}$ representing the known upper bound of $|\hat{\rho}(k)|$; $\star$ induces symmetry. The controller gains are obtained as $F_{k,l} = Y_l G_l^{-1}$, $l \in [1,2]$.

Proof. Substituting (8) into (7) yields

$$\hat{x}(i+1|k) = [\hat{A}_\nu + \hat{B}\delta(i|k)]\hat{x}(i|k) + \hat{D}_\nu w(k+i). \quad (14)$$

Define the Lyapunov function $V(\hat{x}(k)) = \hat{x}(k)^\top P(k)\hat{x}(k)$ with $P(k) = \sum_{l=1}^{2} \alpha_l(k)P_{k,l}$. According to the quadratic boundedness condition (Hu and Ding, 2020), stability of the closed-loop system (14) can be guaranteed by ensuring the set $\Omega = \{\hat{x}(k) \mid \hat{x}(k)^\top P(k)\hat{x}(k) \leq \gamma\}$ as a RPI set. This is realized if the following condition holds for all $i \geq 1$:

$$V(\hat{x}(i|k)) \geq \gamma \implies V(\hat{x}(i+1|k)) \leq V(\hat{x}(i|k)). \quad (15)$$

A sufficient condition of (15) is given as

$$V(\hat{x}(i|k)) \geq \gamma \implies V(\hat{x}(i+1|k)) - V(\hat{x}(i|k)) \leq$$
$$- (\|\hat{x}(i|k)\|_Q^2 + \|\bar{\delta}(i|k)\|_S^2), \ \forall i \geq 1. \quad (16)$$

Since $\|w(k+i)\|^2 \leq w_{\max}$, $V(\hat{x}(i|k)) \geq \gamma$ is equivalent to $V(\hat{x}(i|k)) \geq \gamma w_{\max}^{-1}\|w(k+i)\|^2$. Therefore, the condition (16) is satisfied if there exists a scalar $\xi \in (0,1]$ such that

$$V(\hat{x}(i+1|k)) - (1-\xi)V(\hat{x}(i|k)) + \ell(i|k) \leq 0, \ \forall i \geq 1 \quad (17)$$

where $\lambda = \gamma\xi w_{\max}^{-1}$.

Applying (14) to (17) and reformulating it as a quadratic form of the vector $[\hat{x}(i|k)^\top - w(k+i)^\top]^\top$, then it gives

$$\begin{bmatrix} \Pi_1 & \star \\ \Pi_2 & \Pi_3 \end{bmatrix} \geq 0 \quad (18)$$

where $\Pi_1 = -(\hat{A}_\nu + \hat{B}F(k))^\top P(k+i+1)(\hat{A}_\nu + \hat{B}F(k)) + (1-\xi)P(k+i) - Q - F(k)^\top SF(k)$, $\Pi_2 = \hat{D}_\nu^\top P(k+i+1)(\hat{A}_\nu + \hat{B}F(k))$ and $\Pi_3 = \lambda I - \hat{D}_\nu^\top P(k+i+1)\hat{D}_\nu$.

Applying Schur complement to (18) yields

$$\begin{bmatrix} (1-\xi)P(k+i) & \star & \star & \star & \star \\ 0 & \lambda I & \star & \star & \star \\ \hat{A}_\nu + \hat{B}F(k) & \hat{D}_\nu & P(k+i+1)^{-1} & \star & \star \\ Q^{1/2} & 0 & 0 & I & \star \\ S^{1/2}F(k) & 0 & 0 & 0 & I \end{bmatrix} \geq 0. \quad (19)$$

A sufficient condition of (19) is given as

$$\begin{bmatrix} (1-\xi)P_l & \star & \star & \star & \star \\ 0 & \lambda I & \star & \star & \star \\ \hat{A}_l + \hat{B}F_{k,l} & \hat{D}_l & P_j^{-1} & \star & \star \\ Q^{1/2} & 0 & 0 & I & \star \\ S^{1/2}F_{k,l} & 0 & 0 & 0 & I \end{bmatrix} \geq 0, \ \forall l,j \in [1,2]. \quad (20)$$

Define $X_l = \gamma P_l^{-1}$ and $X_j = \gamma P_j^{-1}$. Substituting $P_l = \gamma X_l^{-1}$ and $P_j = \gamma X_j^{-1}$ into (20) and multiplying both its sides with $\text{diag}\{\gamma^{-1/2}I, \gamma^{-1/2}I, \gamma^{1/2}I, \gamma^{1/2}I, \gamma^{1/2}I\}$ yields

$$\begin{bmatrix} (1-\xi)X_l^{-1} & \star & \star & \star & \star \\ 0 & \xi w_{\max}^{-1} I & \star & \star & \star \\ \hat{A}_l + \hat{B}F_{k,l} & \hat{D}_l & X_j & \star & \star \\ Q^{1/2} & 0 & 0 & \gamma I & \star \\ S^{1/2}F_{k,l} & 0 & 0 & 0 & \gamma I \end{bmatrix} \geq 0, \forall l,j \in [1,2]. \quad (21)$$

There exists a matrix G_l satisfying (Wada et al., 2004)

$$G_l^\top X_l^{-1} G_l \geq G_l^\top + G_l - X_l. \quad (22)$$

Multiplying both sides of (21) with $\text{diag}\{G_l^\top, I, I, I, I\}$ and its transpose, respectively, and using (22) gives (9).

To ensure recursive feasibility, the one-step ahead predicted state $\hat{x}(1|k)$ need to satisfy $\hat{x}(1|k) \in \Omega$. Under Definition 1, this condition holds if Ω is a one-step ahead RPI set for the system (7), i.e.

$$\hat{x}(k+1|k)^\top P(k+1)\hat{x}(k+1|k) \leq \gamma \quad (23)$$

holds under the condition $\|w(k)\|^2 \leq w_{\max}$. Hence, the inequality (23) holds if there is a scalar $\epsilon \in (0,1]$ such that

$$1 - \gamma^{-1}\hat{x}(k+1)^\top P(k+1)\hat{x}(k+1)$$
$$- \epsilon\left[1 - w_{\max}^{-1}w(k)^\top w(k)\right] \geq 0. \quad (24)$$

Applying (7) and (8) to (24), and formulating it in a quadratic form of the vector $[1\ -w(k)^\top]^\top$, then it gives

$$\begin{bmatrix} \hat{\Pi}_1 & \star \\ \hat{\Pi}_2 & \hat{\Pi}_3 \end{bmatrix} \geq 0 \quad (25)$$

where $\hat{\Pi}_1 = 1 - \epsilon - \gamma^{-1}\hat{x}(k)^\top(\hat{A}_\nu + \hat{B}F(k-1))^\top P(k+1)(\hat{A}_\nu + \hat{B}F(k-1))\hat{x}(k)$, $\hat{\Pi}_2 = \gamma^{-1}\hat{D}_\nu^\top P(k+1)(\hat{A}_\nu + \hat{B}F(k-1))\hat{x}(k)$ and $\hat{\Pi}_3 = \epsilon w_{\max}^{-1}I - \gamma^{-1}\hat{D}_\nu^\top P(k+1)\hat{D}_\nu$.

By using Schur complement, (25) holds if

$$\begin{bmatrix} 1 - \epsilon & \star & \star \\ 0 & \epsilon w_{\max}^{-1}I & \star \\ (\hat{A}_l + \hat{B}F_{k-1,l})\hat{x}(k) & \hat{D}_l & \gamma P_j^{-1} \end{bmatrix} \geq 0, \ \forall l, j \in [1, 2].$$

By defining $X_j = \gamma P_j^{-1}$, then (10) is obtained. The constraints $|\delta(k)| \leq \delta_{\max}$ and $|e_{y,k}| \leq e_{y,\max}$ are satisfied if (11) and (12) hold (Hu and Ding, 2020). $\square$

In Theorem 2, the constraint (9) ensures system stability, (10) guarantees recursive feasibility, and (11) - (12) ensure satisfaction of the input and output constraints. Note that the condition (15) holds for $i \geq 1$, rather than $i \geq 0$ as in the existing robust MPC designs (Wada et al., 2004; Zhang et al., 2012). This is because the proposed one-step ahead MPC concerns with the system invariance at the next sampling time $k+1$, while the invariance at time k is already guaranteed at time $k-1$. The implementation of the proposed controller (8) is summarized in Algorithm 1, where $F_{0,l}, l \in [1, 2]$, are solved from the LMI optimization problem in Theorem 2 without (10).

Algorithm 1 One-step ahead robust MPC design for LK

1: Specify ξ, ϵ, Q, S, $\bar{\delta}_{\max}$ and $w_{\max}$.
2: Solve initial gains $F_{0,1}$ and $F_{0,2}$ from the optimization problem in Theorem 2 without (10). Set $k = 1$.
3: Obtain $\hat{x}(k)$ and $\hat{\rho}(k)$, calculate $\alpha_l(k), l \in [1, 2]$, and implement $\delta(k) = \sum_{l=1}^2 \alpha_l(k)F_{k-1,l}\hat{x}(k) + \hat{\rho}(k)$.
4: Solve the controller gains $F_{k+1,l}, l \in [1, 2]$ from the optimization problem in Theorem 2.
5: Save $F_{k,l}, l \in [1, 2]$, set $k = k + 1$ and go to step 3.

3.2 CACC Controller Design

The goal of CACC is to stabilize the platooning error system (3) in the presence of known disturbances a_l and f along with unknown disturbance $\bar{d}$. To remove steady-state offset of the inter-vehicle distance error Δp, the integral $\int \Delta p dt$ is to be used in the CACC controller. Define the new state vector as $\bar{\chi} = [\chi^\top \int \Delta p dt]^\top$. By using (3), then the following discrete-time augmented system is derived:

$$\bar{\chi}(k+1) = \bar{\mathcal{A}}\bar{\chi}(k) + \bar{\mathcal{B}}\varphi(k) + \bar{\mathcal{E}}\bar{\rho}(k) + \bar{\mathcal{E}}\bar{d}(k) \quad (26)$$

with $\bar{\mathcal{A}} = I_3 + t_s \begin{bmatrix} \mathcal{A} & 0 \\ \Gamma & 0 \end{bmatrix}$, $\Gamma = [1 \ 0]$, $\bar{\mathcal{B}} = t_s \begin{bmatrix} \mathcal{B} \\ 0 \end{bmatrix}$, $\bar{\mathcal{E}} = t_s \begin{bmatrix} \mathcal{E} \\ 0 \end{bmatrix}$.

Since $\bar{\rho}(k)$ is known, the following one-step ahead robust MPC controller is designed for the system (26):

$$\varphi(i|k) = \begin{cases} L(k-1)\bar{\chi}(i|k) + \bar{\rho}(i|k), & i = 0 \\ L(k)\bar{\chi}(i|k) + \bar{\rho}(i|k), & \forall i > 0 \end{cases} \quad (27)$$

where $L(k)$ is the controller gain determined at time $k \geq 1$. The controller (27) is designed to minimize the cost function $J_{\text{CACC}}(k) = \sum_{i=1}^\infty \bar{\ell}(i|k)$ with $\bar{\ell}(i|k) = \|\bar{\chi}(i|k)\|_{\bar{Q}}^2 + \|\bar{\varphi}(i|k)\|_{\bar{S}}^2 - \bar{\lambda}\|\bar{w}(k+i)\|^2$ with $\bar{\varphi}(i|k) = L(k)\bar{\chi}(i|k)$, where $\bar{Q}$ and $\bar{S}$ are given positive definite matrices. The controller also ensures the constraints $|\varphi(k)| \leq \varphi_{\max}$ and $|\Delta p(k)| \leq$

$\Delta p_{\max}$, where $\varphi_{\max}$ and $\Delta p_{\max}$ are the maximum desired torque and inter-vehicle distance error, respectively.

By setting $\alpha_1 = 1$ and $\alpha_2 = 0$, the CACC system (26) and controller (27) are in similar forms of the LK system (7) and controller (8), respectively. Hence, following Theorem 2 in Section 3.1 with $\bar{X} = \bar{X}_1 = \bar{X}_2 = \bar{G}_1 = \bar{G}_2$, the controller gain $L(k) = \bar{Y}\bar{X}^{-1}$ is solved from the LMI optimization problem below:

$$\min_{\bar{\gamma}, \bar{X}, \bar{Y}} \bar{\gamma}$$

$$\begin{bmatrix} (1-\bar{\xi})\bar{X} & \star & \star & \star & \star \\ 0 & \bar{\xi}\bar{d}_{\max}^{-1}I & \star & \star & \star \\ \bar{\mathcal{A}}\bar{X} + \bar{\mathcal{B}}\bar{Y} & \bar{\mathcal{E}} & \bar{X} & \star & \star \\ \bar{Q}^{1/2} & 0 & 0 & \bar{\gamma}I & \star \\ \bar{S}^{1/2}\bar{Y} & 0 & 0 & 0 & \bar{\gamma}I \end{bmatrix} \geq 0 \quad (28)$$

$$\begin{bmatrix} 1-\bar{\epsilon} & \star & \star \\ 0 & \bar{\epsilon}\bar{d}_{\max}^{-1}I & \star \\ (\bar{\mathcal{A}}\bar{X} + \bar{\mathcal{B}}L(k-1))\bar{\chi}(k) & \bar{\mathcal{E}} & \bar{X} \end{bmatrix} \geq 0 \quad (29)$$

$$\begin{bmatrix} \bar{\varphi}_{\max}^2 I & \star \\ \bar{Y}^\top & \bar{X} \end{bmatrix} \geq 0 \quad (30)$$

$$\begin{bmatrix} \Delta p_{\max}^2 I & \star & \star \\ (\bar{\mathcal{A}}\bar{X} + \bar{\mathcal{B}}\bar{Y})^\top \bar{\Gamma}^\top & \bar{X} & \star \\ \bar{\mathcal{E}}^\top \bar{\Gamma}^\top & 0 & \bar{d}_{\max}^{-1}I \end{bmatrix} \geq 0 \quad (31)$$

$$\bar{\gamma} > 0, \ \bar{X} = \bar{X}^\top > 0 \quad (32)$$

where $\bar{\Gamma} = [1 \ 0 \ 0]$; $\bar{\xi}, \bar{\epsilon} \in (0, 1]$; $\bar{\varphi}_{\max} = \varphi_{\max} - (ma_{\max}^l + f_{\max})$ with the known upper bounds $a_{\max}^l$ and $f_{\max}$ of $|a^l(k)|$ and $|f(k)|$, respectively.

4. CASE STUDY

A platoon of three vehicles is used to verify the proposed design. All the vehicles have the same parameters: $m = 1650$ kg, $g = 9.8$ m/s^2, $I_z = 2315.3$ kg $\cdot$ m^2, $l_f = 1.11$ m, $l_r = 1.59$ m, $c_f = 66500$ N, $c_r = 49400$ N, $\mu = 0.015$, $A_f = 2.031$ m^2, $C_d = 0.32$, $\rho_{\text{air}} = 1.2$ kg/m^3, $d_r = 10$ m, $t_s = 0.05$ s, $v_{\min} = 10$ m/s, $v_{\max} = 40$ m/s, $\delta_{\max} = 10$ deg, $\varphi_{\max} = 6000$ N, $\Delta p_{\max} = 5$ m, $e_{y,\max} = 0.5$ m.

The followers use the same LK controller designed from Theorem 2 with $\xi = \epsilon = 0.01$, $Q = 10^2 \times I_5$ and $S = 10$. They also use the same CACC controller determined by solving the LMI optimization problem in Section 3.2 with $\bar{\xi} = \bar{\epsilon} = 0.01$, $\bar{Q} = 10^8 \times I_3$ and $\bar{S} = 1$.

To validate the design efficacy within the entire velocity range $[v_{\min}, v_{\max}]$ and under variable road geometry, the profiles of leader velocity v_l, road curvature $1/R$, bank angle θ and grade angle β in Fig. 1 are considered. The wind speed v_{wind} takes random values within $[-1, 1]$ m/s. The leader has the initial state $(p^l(0), v^l(0)) = (17, 10)$. Follower 1 has the initial state $(p(0), v(0)) = (12, 10)$ and $(e_y(0), \dot{e}_y(0), e_\psi(0), \dot{e}_\psi(0)) = (0.2, 0, 0, 0)$. Follower 2 has the initial state $(p(0), v(0)) = (0, 10)$ and $(e_y(0), \dot{e}_y(0), e_\psi(0), \dot{e}_\psi(0)) = (0.1, 0, 0, 0)$.

The proposed MPC is compared with the existing real-time MPC (Zhang et al., 2012). For fair comparison, the feedback controller in Zhang et al. (2012) is modified to combine feedforward and feedback actions in a similar form as the proposed MPC. Results of the inter-vehicle distance, lateral displacements and steering angles under

the two MPC designs are depicted in Fig. 3. From the two top subplots, it is seen that under both designs, the inter-vehicle distances of Leader & Follower 1 and Followers 1&2, are controlled to be the desired value d_r, while the errors Δp are within the given set $[-\Delta p_{max}, \Delta p_{max}]$. However, the inter-vehicle distances using the real-time MPC have bigger overshoots. From the two middle subplots, it is observed that both designs achieve almost the same lateral displacement response. Although small displacements exist in the presence of road curvature and bank, they are within the given set $[-e_{y,max}, e_{y,max}]$. However, there are oscillations in the lateral displacements under the real-time MPC, so are the the steering angles in the two bottom subplots. The results above demonstrate that the proposed MPC achieves stable CACC and LK by using the one-step ahead design. However, the real-time MPC has fluctuations in the steering angle commands, leading to undesired driving comfort.
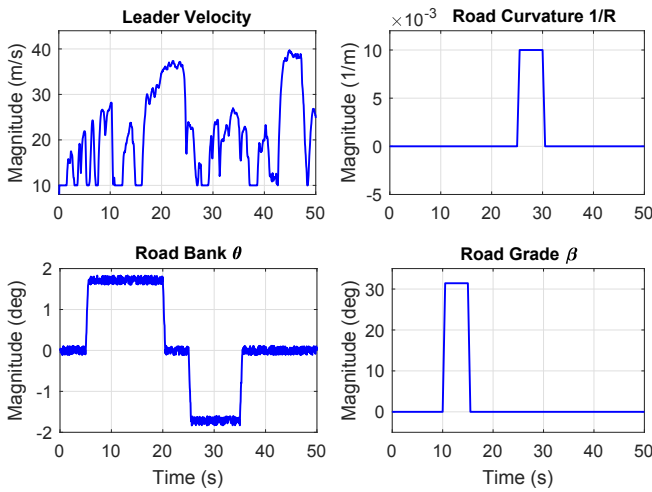
Fig. 2. Profiles of leader velocity and road geometry
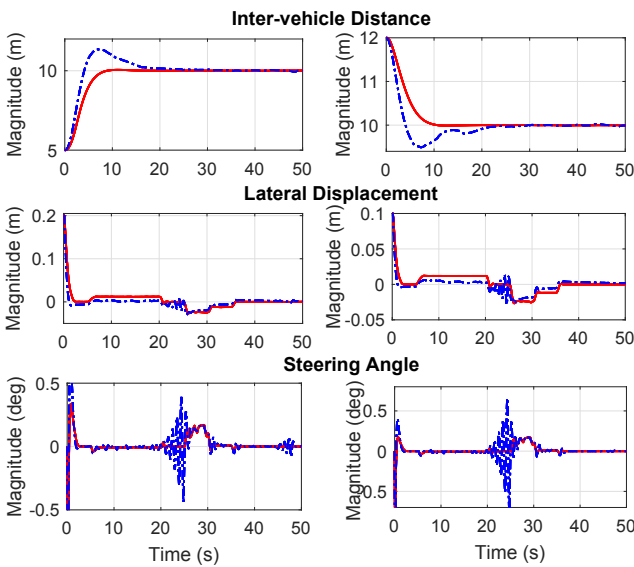
Fig. 3. Responses of inter-vehicle distance, lateral displacement and steering angle (Red solid line: proposed MPC; Blue dash-dot line: real-time MPC.)

5. CONCLUSION

A one-step ahead robust MPC is proposed for achieving stable CACC and LK under variable road conditions, and avoiding the online computational delay. The design efficacy is validated by platooning of three vehicles under time-varying leader velocity and road geometry. The results show that the proposed MPC achieves more robust platooning and better driving performance than the traditional real-time MPC. Future research will consider verifying the design via hardware-in-the-loop tests.

REFERENCES

Attia, R., Orjuela, R., et al. (2012). Coupled longitudinal and lateral control strategy improving lateral stability for autonomous vehicle. In *Proc. ACC*, 6509–6514. IEEE.

Blanchini, F. and Miani, S. (2008). *Set-theoretic methods in control*. Springer.

Daafouz, J. and Bernussou, J. (2001). Poly-quadratic stability and H_∞ performance for discrete systems with time varying uncertainties. In *Proc. CDC*, 267–272. IEEE.

Feng, S., Sun, H., et al. (2019). Tube-based discrete controller design for vehicle platoons subject to disturbances and saturation constraints. *IEEE Trans. Control Syst. Technol.* doi:10.1109/TCST.2019.2896539.

Findeisen, R. and Allgöwer, F. (2004). Computational delay in nonlinear model predictive control. *IFAC Proc.*, 37(1), 427–432.

Firoozi, R., Nazari, S., et al. (2019). Safe adaptive cruise control with road grade preview and V2V communication. In *Proc. ACC*, 4448–4453. IEEE.

Guanetti, J., Kim, Y., et al. (2018). Control of connected and automated vehicles: State of the art and future challenges. *Annu. Rev. Control*, 45, 18–40.

Gupta, A. and Falcone, P. (2018). Low-complexity explicit MPC controller for vehicle lateral motion control. In *Proc. ITSC*, 2839–2844. IEEE.

Hu, J. and Ding, B. (2020). One-step ahead robust MPC for LPV model with bounded disturbance. *Eur. J. Control*, 52, 59–66.

Rajamani, R. (2011). *Vehicle dynamics and control*. Springer.

van Nunen, E., Reinders, J., et al. (2019). String stable model predictive cooperative adaptive cruise control for heterogeneous platoons. *IEEE Trans. Intell. Veh.*, 4(2), 186–196.

Wada, N., Saito, K., et al. (2004). Model predictive control for linear parameter varying systems using parameter dependent Lyapunov function. In *Proc. MWSCAS*, volume 3, 133–136. IEEE.

Xu, L., Zhuang, W., et al. (2019). Modeling and robust control of heterogeneous vehicle platoons on curved roads subject to disturbances and delays. *IEEE Trans. Veh. Technol.*, 68(12), 11551–11564.

Zavala, V.M. and Biegler, L.T. (2009). The advanced-step NMPC controller: Optimality, stability and robustness. *Automatica*, 45(1), 86–93.

Zhang, D., Li, K., et al. (2012). A curving ACC system with coordination control of longitudinal car-following and lateral stability. *Vehicle Syst. Dyn.*, 50(7), 1085–1102.